

Numerical simulation of a passive scalar transport in a jet flow

Nabil MRABTI¹, Zouhaier HAFSIA², Ghazi BELLAKHAL³ and Jamel CHAHED⁴
⁽¹⁻³⁾ ENIT. Laboratoire d'Hydraulique B.P. 37. Le Belvédère, 1002 Tunis, Tunisia

E-mail : ⁽¹⁾ Mrabti.Nabil@gmail.com ⁽²⁾ Zouhaier.Hafsia@enit.rnu.tn
⁽³⁾ Ghazi.Bellakhal@enit.rnu.tn ⁽⁴⁾ Jamel.Chahed@enit.rnu.tn

ABSTRACT - The aims of the present study is the validation of the turbulent transport of a passive scalar in a jet flow with the CFD code "PHOENICS". The first stage of this work is the analysis and modelling of jet flow. We are interested in particular in two important questions in this validation flow case. The first question is relative to the sensitivity of numerical results to the initial conditions of the turbulent kinetic energy and the dissipation rate at the entry of the jet. We test different conditions, in particular those proposed by Chen and al. (1979). The second question concerns the analysis of the Rodi and al. (1980) adjustment of the standard (k,ε) constants for its appropriate application to the circular jet flow. We compare the standard (k,ε) model and the adjusted (k,ε) model that we have implemented in the PHOENICS code. The numerical results are confronted to the experimental results of Hu and al. (2000) associated to the near flow field. The comparison between simulated and experimental results show that the mean velocity, turbulence intensity and concentration are improved by Chen and Rodi Adjustments. However the simulated concentration profiles remain different from the experimental results.

1- INTRODUCTION

During the last decades, an important progress in the field of Computational Fluid Dynamic has been achieved. The application of the CFD code made it possible to apprehend significant difficulties which persist in the optimisation and the control of transport processes. Also evident is the ambition to use CFD for more and more challenging problems covering different flow features. However, it is advantageous to review simple cases for the validity of the numerical results.

The jet flow is a simple case which was widely studied. Fischer and al. (1979) were interested to the zone of established flow where self similar behaviour was proved. Turbulent round jets have also received significant attention in the literature, including Wygnanski (1969) and List (1982).

More recently, the optical techniques advances such as PIV (Particle Image Velocimetry) and PLIF (Planar Induced Laser Fluorescence) have provided new opportunities for the non-intrusive simultaneous acquisition of multiple flow variables (Hu and al. (2000)).

To describe turbulence in jet flows, we generally use in CFD code the two equations (k-ε) closure model for the prediction of mean and turbulent fields. Despite of its frequent use for the prediction of the hydrodynamics of the jet, much of authors showed that the standard version of

the (k-ε) model is insufficient. In fact, Chen and al. (1979) showed that it is necessary to adjust turbulence conditions at the entry with Gaussian profiles. Then, Rodi and al. (1980) showed that the constants of the model are not applicable directly to the circular jet flow and that they could depend on the deceleration velocity on the jet axis. They have, for this purpose, suggested adjustments for the determination of the constants of the (k-ε) model for the circular jet. These adjustments is introduced in the PHOENICS code and numerical results is compared to the experimental results of Hu and al. (2000) associated to the near field of the jet flow.

2- PASSIVE SCALAR TRANSPORT EQUATIONS IN A JET FLOW

2-1 Jet flow characteristics

In this work, we study a single phase jet transporting a passive scalar : a concentration. The flow field has a symmetry of revolution and hence the flow is bidimensionnel. The figure (1) shows the studied case:

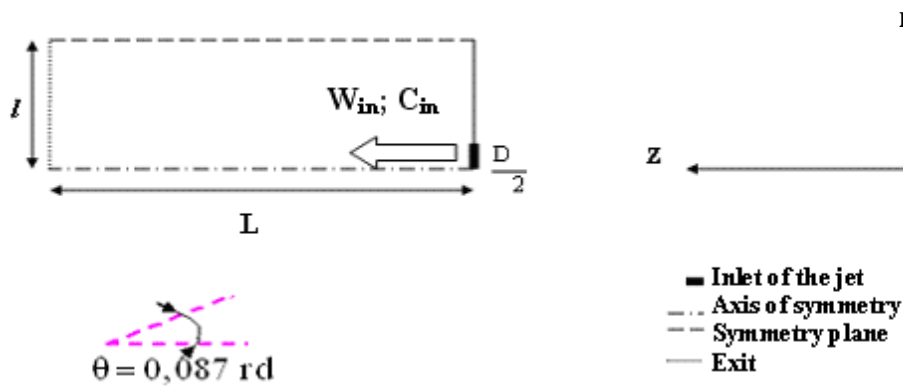


Figure1 : Geometry of the jet flow domain

The geometry of the problem is defined by : the width $l = 10 \cdot D$ and the length $L = 30 \cdot D$ where D is the diameter of the nozzle : $D = 30$ mm. The inlet velocity is $U_0 = 0.20$ m/s corresponding to a Reynolds number of 6000. To describe the transport of the concentration we take the Prandtl number equal to 0.7.

2-2 Mathematical Model

For a stationary single-phase flow and with negligible buoyancy force, the averaged equations describing turbulent flow can be written in cylindrical coordinates (r : radial direction and z longitudinal direction) as the following general form :

$$\frac{1}{r} \left[\frac{\partial (r \rho \phi W)}{\partial z} + \frac{\partial (r \rho V \phi)}{\partial r} \right] = \frac{1}{r} \left[\frac{\partial}{\partial z} \left(r \Gamma_{\phi} \frac{\partial \phi}{\partial z} \right) + \frac{\partial}{\partial r} \left(r \Gamma_{\phi} \frac{\partial \phi}{\partial r} \right) \right] + S_{\phi} \quad (1)$$

Where: ρ is the fluid density; Φ is a general dependant variable; W and V are the mean velocities and Γ_{ϕ} is a diffusive exchange coefficient.

The left hand term represent convection transport; the first term in the right hand represent diffusion and S_{ϕ} is a source terme.

The turbulence model closure is the (k – ε) model where the turbulent dynamic viscosity is :

$$\mu_t = C_\mu \rho \frac{k^2}{\varepsilon} \quad (2)$$

Table 1 : Summary of transport equations

<i>Equation</i>	Φ	Γ_Φ	S_Φ
Conservation of mass	1	0	0
Axial momentum	W	$\mu_e = \mu + \mu_t$	$\frac{\partial P}{\partial z} + \frac{\partial}{\partial z} \left[(\mu + \mu_t) \frac{\partial W}{\partial z} \right] + \frac{1}{r} \frac{\partial}{\partial r} \left[(\mu + \mu_t) \frac{\partial V}{\partial z} \right]$
Radial momentum	V	$\mu_e = \mu + \mu_t$	$-\frac{\partial P}{\partial r} + \frac{\partial}{\partial z} \left[(\mu + \mu_t) \frac{\partial W}{\partial r} \right] + \frac{1}{r} \frac{\partial}{\partial r} \left[(\mu + \mu_t) \frac{\partial V}{\partial r} \right] - 2(\mu + \mu_t) \frac{V}{r^2}$
Turbulent kinetic energy	k	$\mu + \frac{\mu_t}{\sigma_k}$	Pr od – ρε
Dissipation rate	ε	$\mu + \frac{\mu_t}{\sigma_\varepsilon}$	$\frac{\varepsilon}{k} (C_{1\varepsilon} \text{Pr od} - C_{2\varepsilon} \rho \varepsilon)$
Concentration	C	$\mu + \frac{\mu_t}{\sigma_C}$	0

$$\text{Pr od} = (\mu + \mu_t) \left[2 \left(\left(\frac{\partial W}{\partial z} \right)^2 + \left(\frac{\partial V}{\partial r} \right)^2 + \left(\frac{V}{r} \right)^2 \right) + \left(\frac{\partial W}{\partial r} + \frac{\partial V}{\partial z} \right)^2 \right] : \text{Production of kinetic energy.}$$

μ : Dynamic viscosity; σ_k , σ_ε and σ_c are turbulent Prandtl numbers respectively of k, ε and C given by : $\sigma_k = 1.00$, $\sigma_\varepsilon = 1.30$, $\sigma_c = 0.7$. The empirical constants of (k – ε) standard turbulence model are given by : $C_\mu = 0.09$; $C_{1\varepsilon} = 1.44$ and $C_{2\varepsilon} = 1.92$

2-3 Boundary conditions

a) Inlet

Chen and al. (1979) proposed to change the inlet boundary condition relative to velocity profiles as a flat profile or as a triangular profile following the jet entry characteristics. For the turbulent kinetic energy and the dissipation rate, they adopted a Gaussian profiles at the inlet :

$$k = k_{in} \exp[-1.7 r^2] \quad 0 < r < \frac{D}{2} \quad (3)$$

$$\varepsilon = \varepsilon_{in} \exp[-1.7 r^2] \quad 0 < r < \frac{D}{2} \quad (4)$$

k_{in} and ε_{in} are respectively the kinetic energy and the dissipation rate at the inlet. They are given by the relations :

$$k_{in} = \alpha_k W_{in}^2 \quad (5)$$

$$\varepsilon_{in} = \alpha_\varepsilon \frac{W_{in}^3}{d} \quad (6)$$

Where W_{in} is the inlet axial velocity.

The coefficients α_k and α_ε are adjusted numerically in order to reproduce the experimental data.

b) Boundary conditions on the axis of the jet

Boundary conditions on the axis of the jet are Neumann type with negligible normal gradients for the longitudinal component of the W velocity, the turbulent kinetic energy k , the dissipation rate and the concentration C :

$$\frac{\partial}{\partial r}(W, k, e, C) = 0 \quad (7)$$

2-4 The (k-ε) adjustments for near field jet flow

The standard $(k-\varepsilon)$ model, previously described, has been applied with success in a different flow configurations but its constants is not universal. The application field of this model can be extended if its constants are substituted by functions of the flow parameters. In this context, Rodi and al. (1980) proposed to replace the $(k-\varepsilon)$ constants by the following equations :

$$C_\mu = 0.09 - 0.04 f \quad (8)$$

$$C_{2\varepsilon} = 1.92 - 0.0667 f \quad (9)$$

Where:

$$f = \left[\frac{\delta}{\Delta W_{max}} \left(\frac{\partial W_c}{\partial z} - \left| \frac{\partial W_c}{\partial z} \right| \right) \right]^{0.2} \quad (10)$$

With:

ΔW_{max} : Maximal velocity

$\delta = r_e - r_c$: (c: center and e: ambient fluid)

So, equation (13) can be written as :

$$C_\mu = 0.09 - 0.04 * \left[\frac{r_{1\%}}{W_c} \left(\left(\frac{\partial W_c}{\partial z} \right) - \left| \frac{\partial W_c}{\partial z} \right| \right) \right]^{0.2} \quad (11)$$

With W_c the longitudinal mean velocity on the axis of the jet and $r_{1\%}$ the width of the jet where W is equal to 1% W_c .

In this expression the gradient of velocity term is approximated by the difference method :

$$\frac{\partial W_c}{\partial z} \approx \frac{W_i - W_{i-1}}{z_i - z_{i-1}} \quad (12)$$

Source term, in the transport equation of the dissipation rate is linearized by the Newton-Raphson method :

$$S_e = C_e (V_e - e) + C_{1e} e n_t \frac{E}{k} \quad (13)$$

E is the strain rate defined by :

$$E = \frac{(U_{i,j} + U_{j,i})^2}{2} \quad (14)$$

Where:

$$C_e = 4 * C_{2e} * \frac{e}{(3k)} \quad (15)$$

$$V_e = \frac{e}{4} \quad (16)$$

Thus, we can modify directly the source term of the dissipation rate by introducing a new constant formulation :

$$C_{2e} = 1.92 - 0.0677 * \left[\frac{r_{1\%}}{W_c} \left(\left(\frac{\partial W_c}{\partial z} \right) - \left| \frac{\partial W_c}{\partial z} \right| \right) \right]^{0.2} \quad (17)$$

These formulations is introduced in the PHOENICS code by "PLANT" technique which is an attachment to the PHOENICS-SATELLITE that allows to simplify the integration of the user coding through the Q1 file.

Figures (2 and 3) present respectively the longitudinal evolution of the coefficients C_m and C_{2e} following the Rodi adjustments. The value of C_m coefficient is always lower to 0,09. In the zone close to the jet entry ($z < 8D$), C_m decrease toward a minimal value of 0,0866. The value of C_{2e} remain lower to 1,92.

3- RESULTS AND DISCUSSIONS

We compare the mean velocity, turbulence intensity and concentration profiles at 2D, 3D and 4D on the near flow field with experimental measurements of Hu and al. (2000).

Preliminary numerical tests show that the following values of the turbulence levels improve the hydrodynamic field of the jet flow : $\alpha_k = 0.01$ and $\alpha_\epsilon = 0.006$.

3-1 Mean velocity profiles

Figures (4-a), (4-b) and (4-c) present the simulated and experimental profiles of mean velocity respectively at three sections near the jet entry. The jet expansion is well reproduced by the standard (k- ϵ) model and the adjusted (k- ϵ) model for the three sections considered. However, the standard (k- ϵ) model does not predict correctly the velocity attenuation with different levels of kinetic energy and dissipation rate at the jet entry (constant levels). The numerical simulations with the adjusted (k- ϵ) model and with Chen profiles at the jet entry indicates a good concordance with the experimental results of Hu and al. (2000) at sections $Z = 3D$ and $Z = 4D$. At section $Z = 2D$, the difference between the experimental and numerical results can be assigned to the anisotropy of velocity fluctuations in vicinity of the jet entry.

3-2 Turbulence intensity profiles

Figures (5-a), (5-b) and (5-c) show the velocity fluctuations profiles which represent the

turbulence intensity respectively at the three sections considered. With the adjusted (k- ϵ) model, the turbulence intensity is better reproduced on the jet axis at sections $Z = 3D$ and $Z = 4D$. The two turbulence models reproduce the same value of the maximal turbulence intensity corresponding to the maximal production.

3-3 Concentration profiles

Figures (6-a), (6-b) and (6-c) show the simulated concentration profiles with the two (k- ϵ) turbulence models and the experimental results respectively at the three sections considered. The Rodi and Chen adjustments has the tendency to better predict the concentration on the jet axis and the expansion of the concentration for the three sections. However, the simulated concentration profiles with Rodi and Chen adjustments remain different from the experimental results.

4- Conclusion

It is clear that the modifications of the constants of the standard (k- ϵ) model proposed by Rodi with the Chen profiles at the entry of a circular jet implies a significant improvements of the predictions of the average turbulence fields and turbulence intensity essentially at sections $Z = 3D$ and $Z = 4D$. At section $Z = 2D$, the difference between the experimental and numerical results can be assigned to the anisotropy of velocity fluctuations in vicinity of the jet entry. The confrontation of the experimental and numerical results shows that these adjustments suggested by Chen and Rodi improves the concentration profiles near the jet entry at three sections. However the simulated concentration profiles remain different from the experimental results.

The scalar transport model based on a direct proportionality between diffusivities of momentum and the passive scalar appears insufficient. In fact, many authors such us Faeth and al. (1995) showed that the Schmidt number is variable through the cross-section of the jet flow. To better improve the hydrodynamic in vicinity of the jet entry (at $Z = 2D$), we can use a Reynolds Stress Model which can reproduce the anisotropy of velocity fluctuations.

REFERENCES

- [1] Chen C.J. et Constantinou P.N., (1979), "On the near field characteristics of axisymmetric turbulent buoyant jets in a uniform environment", Int. J. Heat Mass Transfer, Vol. 22, pp. 245-255.
- [2] Chen C.J., Rodi W., (1980), "Vertical turbulent buoyant jets", A review of Experimental data, Pergamon Press, Oxford, p.16.
- [3] Faeth G.M., (1995), "Self preserving buoyant turbulent plumes", Fluid Mech. of Fires- A symposium in Honour of Prof. Edward Edom Zukoski, pp. 275-284.
- [4] Fischer H.B., List E.J., Koh R.C.Y., Imberger J. et Brooks N.H., (1979), "Mixing in inland and coastal waters", Academic Press, New York.
- [5] HU H., SAGA T., KOBAYASHI T., TANIGUCHI N., CHEN Y., CHIO S. and Narahara K.,(2000), "Simultaneous Velocity and Concentration Measurements in a

- Turbulent Jet Flow by Using PIV-PLIF Combined System”, Proceedings of the 4th JSME-KSME Thermal Engineering Conference, October 1-6, 2000, Kobe, Japan.
- [6] Lemoine F., Antoine Y. et Lebouché M., (2001) "Turbulent transport of a passive scalar in a round jet discharging into a co-flowing stream", *Eur. J. Mech. B - Fluids* Vol. 20 PP. 275–301.
 - [7] List E.J., (1982), "Turbulents jets and plumes", *Ann. Rev. Fluid Mech.*, Vol.14, pp. 189-212.
 - [8] Rodi W., (1980), "Turbulence models and their application in hydraulics", A state of art review.
 - [9] Wygnanski I. et Fielder H., (1969), "Some measurements in the self-preserving jet", *J. Fluid Mech.*, Vol.38, pp. 577-612.

(1) Evolution of the(k-e) turbulence model constants:

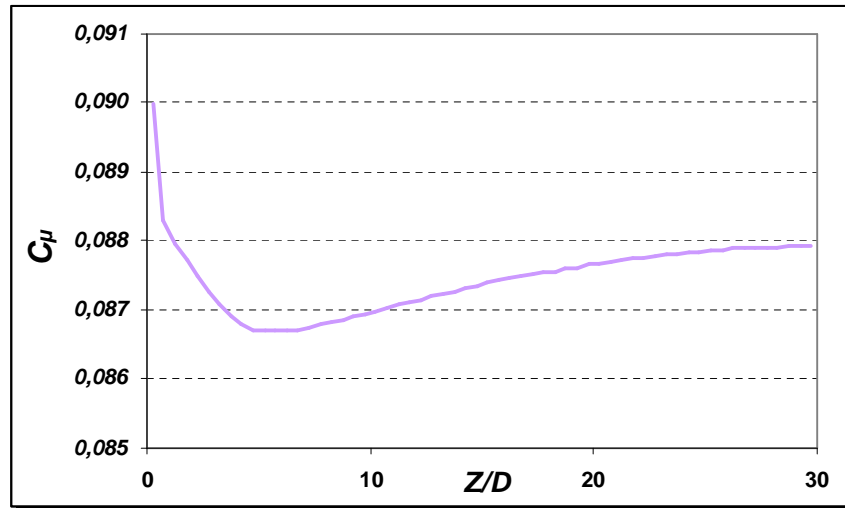


Fig.(2) : Longitudinal evolution of C_μ .

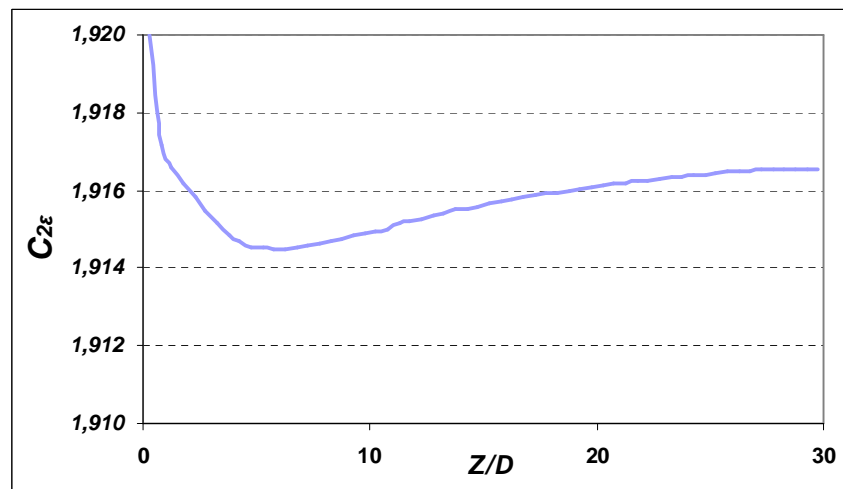


Fig.(3) : Longitudinal evolution of C_{2e} .

(2) Mean velocity profiles:

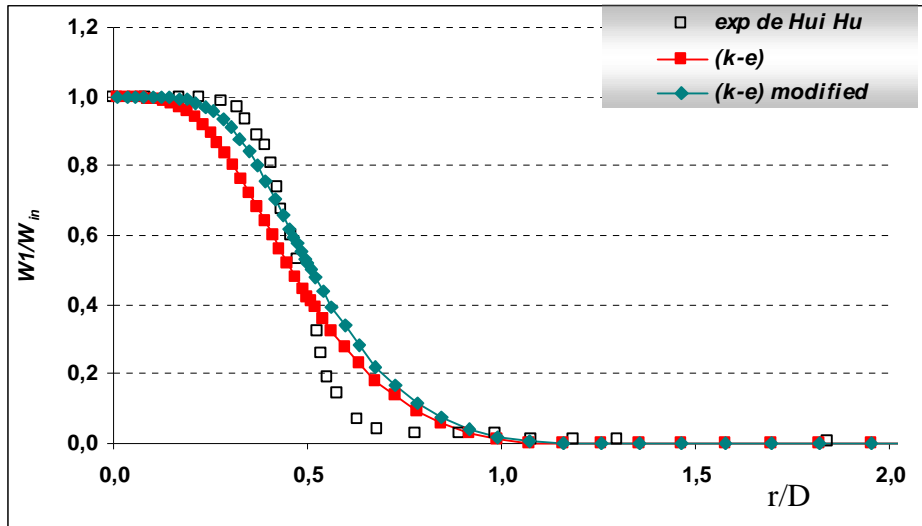


Fig.(4-a) : Mean velocity Profile at : $Z = 2D$.

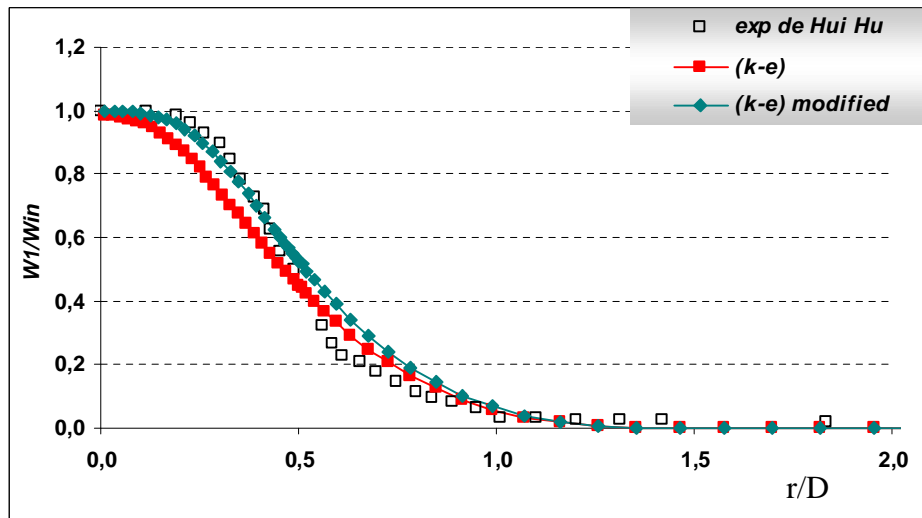


Fig.(4-b) : Mean velocity Profile at : $Z = 3D$.

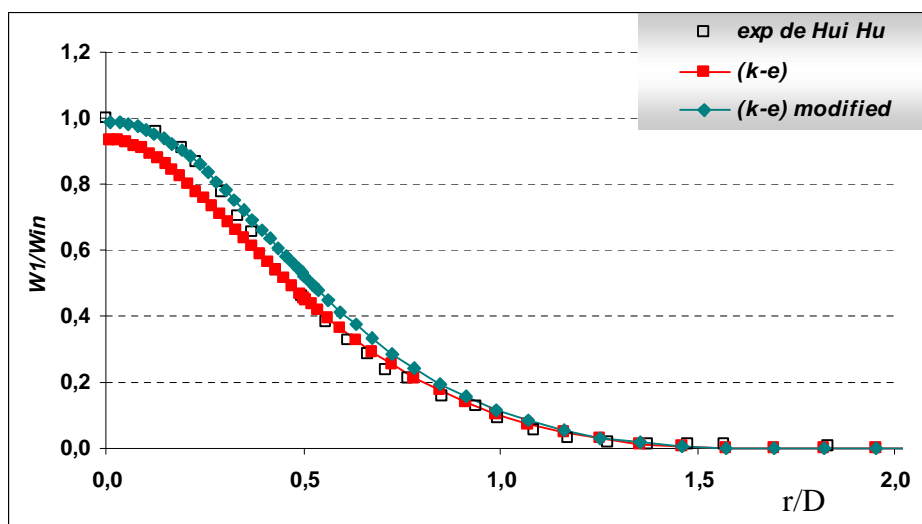


Fig.(4-c) : Mean velocity Profile at : $Z = 4D$.

(3) *Turbulence intensity profiles:*

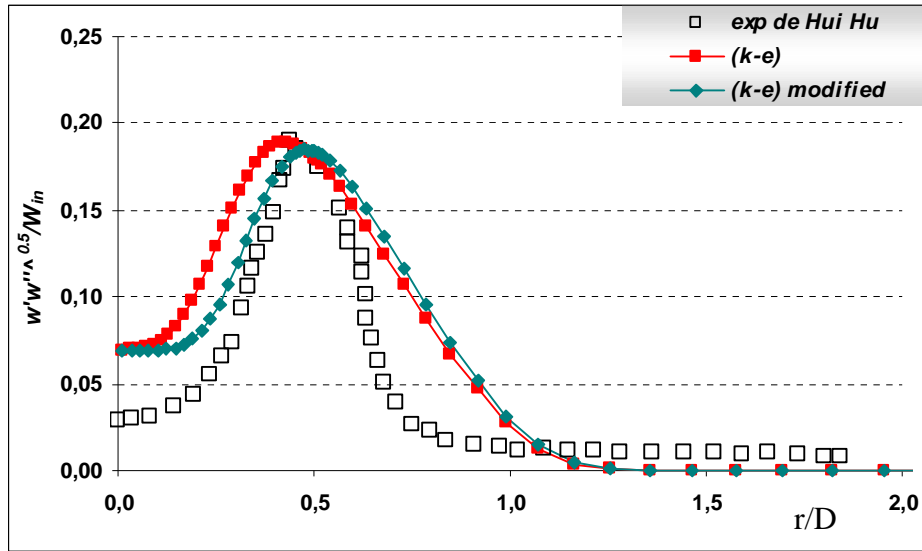


Fig.(5-a) : Velocity fluctuations profiles at $Z = 2D$.

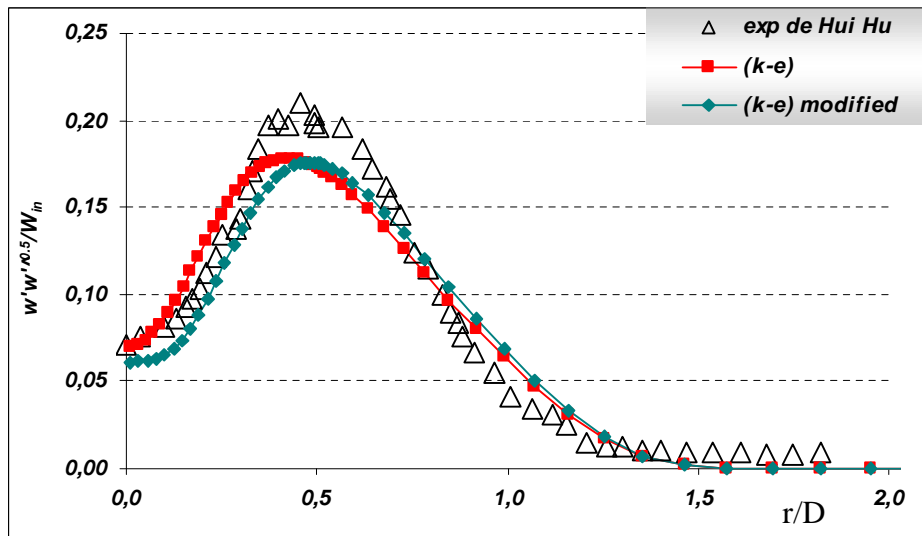


Fig.(5-b) : Velocity fluctuations profiles at $Z = 3D$.

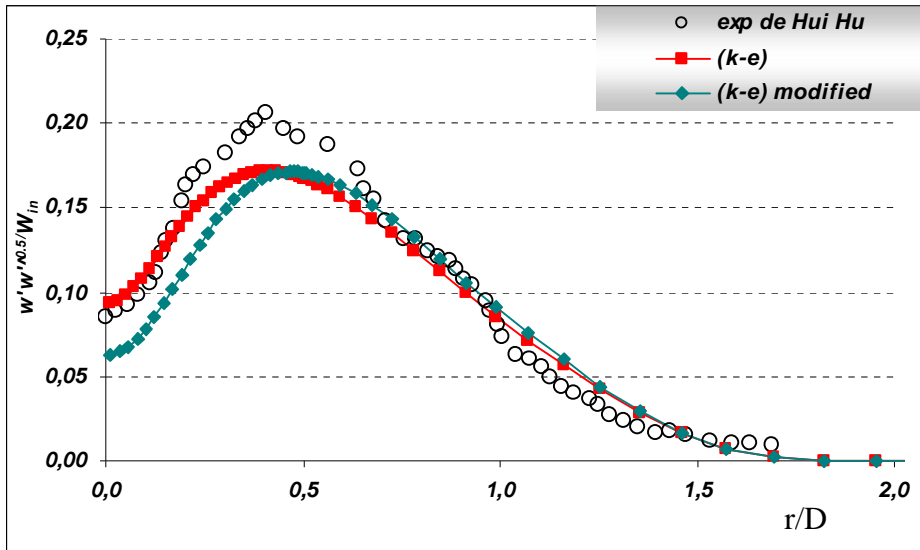


Fig.(5-c) : Velocity fluctuations profiles at $Z = 4D$.

(4) Concentration profiles:

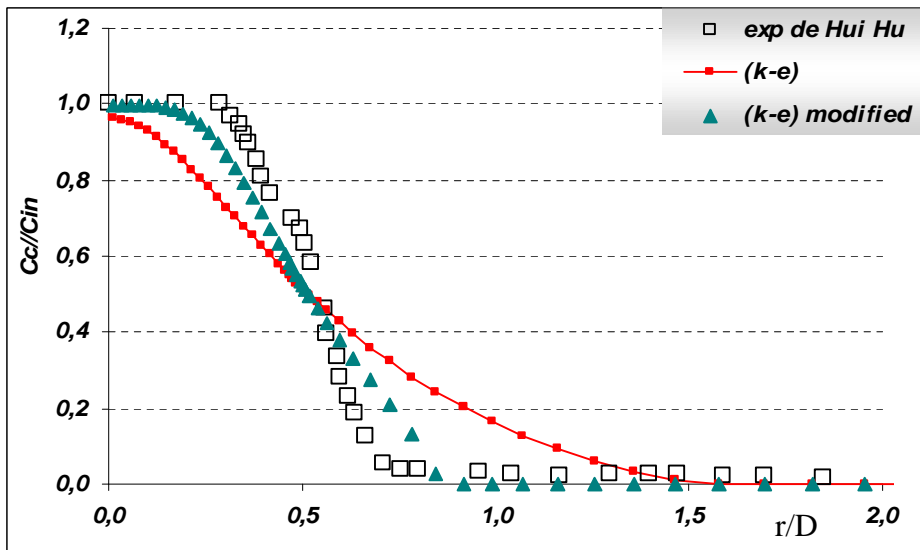


Fig.(6-a) : Concentration profiles at $Z = 2D$

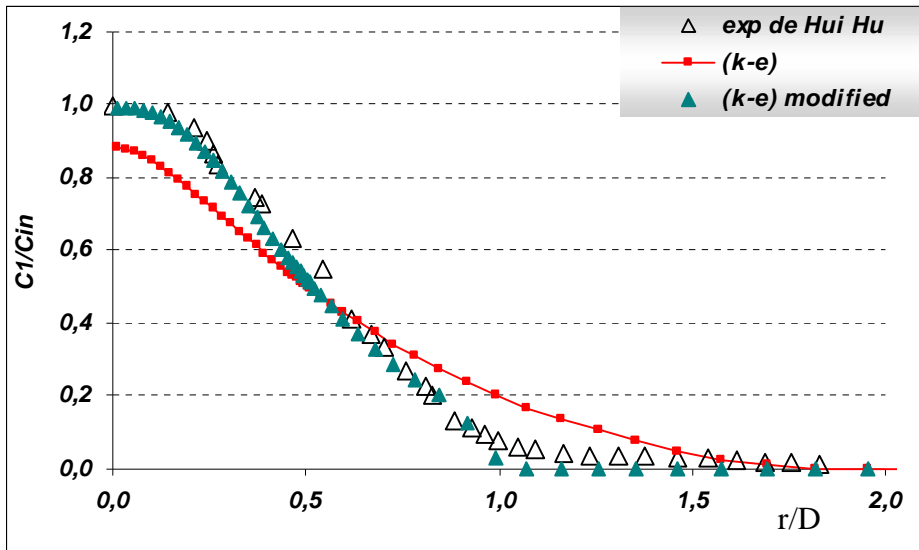


Fig.(6-b) : Concentration profiles at $Z = 3D$

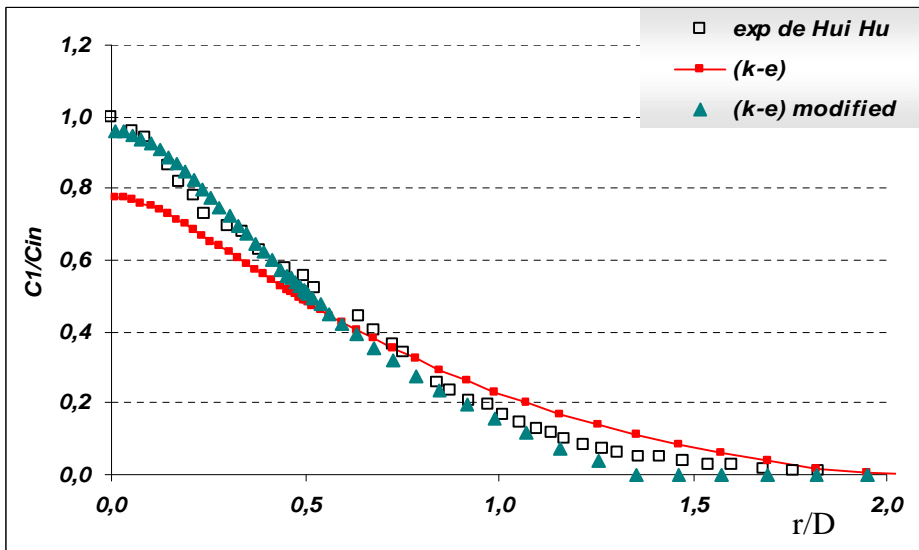


Fig.(6-c) : Concentration profiles at $Z = 4D$